

Document downloaded from:

<http://hdl.handle.net/10251/68450>

This paper must be cited as:

Pérez-Esteve, É.; Fuentes López, A.; Coll Merino, MC.; Acosta, C.; Bernardos Bau, A.; Amoros Del Toro, P.; Marcos Martínez, MD.... (2015). Modulation of folic acid bioaccessibility by encapsulation in pH-responsive gated mesoporous silica particles. *Microporous and Mesoporous Materials*. 202:124-132. doi:10.1016/j.micromeso.2014.09.049.



The final publication is available at

<https://dx.doi.org/10.1016/j.micromeso.2014.09.049>

Copyright Elsevier

Additional Information

1 ***Modulation of folic acid bioaccessibility by encapsulation in pH-responsive***
2 ***gated mesoporous silica particles***

3
4 Édgar Pérez-Esteve^a, Ana Fuentes^a, Carmen Coll^{b,c}, Carolina Acosta^a, Andrea Bernardos^{a,b}, Pedro
5 Amorós^d, María D. Marcos,^{b,c} Félix Sancenón^{b,c}, Ramón Martínez-Máñez^{b,c,*}, José M. Barat^a

6
7 ^aGrupo de Investigación e Innovación Alimentaria, Universitat Politècnica de València. Camino de
8 Vera s/n, 46022, Spain

9 ^bCentro de Reconocimiento Molecular y Desarrollo Tecnológico (IDM), Unidad Mixta Universitat
10 Politècnica de València – Universidad de Valencia. Departamento de Química Universitat
11 Politècnica de València, Camino de Vera s/n, 46022, Valencia, Spain

12 ^cCIBER de Bioingeniería, Biomateriales y Nanomedicina (CIBER-BBN)

13 ^dInstitut de Ciència dels Materials (ICMUV), Universitat de València, P.O. Box 2085, 46071,
14 Valencia, Spain

15 * Corresponding author: Tel.: +34 963877343; E-mail address: rmaez@qim.upv.es (R. Martínez-
16 Máñez).

17
18 **ABSTRACT**

19 A study on the controlled release of Folic Acid (FA) from pH-responsive gated mesoporous silica
20 particles (MSP) is reported. The MCM-41 support was synthesized using tetraethyl orthosilicate
21 (TEOS) as hydrolytic inorganic precursor and the surfactant hexadecyltrimethylammonium
22 bromide (CTAB) as porogen species. Calcination of the mesostructured phase resulted in the
23 starting solid. This solid was loaded with FA to obtain the initial support **S0**. Moreover, this FA-
24 loaded material was further functionalized with 3-[2-(2-
25 aminoethylamino)ethylamino]propyltrimethoxysilane (N3) in order to obtain the gated
26 polyamine-functionalised material **S1**. Solids **S0** and **S1** were characterized using standard solid
27 state procedures. It was found that the functionalization process and the inclusion of FA on the
28 pores do not modify the mesoporous structure of the starting material. FA delivery studies in
29 water with solids **S0** and **S1** were carried out in water at pH 2 and 7.5. **S0** was not able to
30 completely inhibit FA delivery at acidic pH yet a rapid FA release at neutral pH was observed in
31 few minutes. In contrast, **S1** was tightly capped at pH 2 and displayed a sustained delivery of FA
32 when the pH was switched to 7.5. In the second part of the study, FA loading and
33 functionalization of **S1**-like supports was optimized. In particular, solids loaded with FA in
34 phosphate buffered saline (PBS) and capped with N3 in acetate buffer at pH 2 exhibited a delivery
35 capacity up to 95 µg FA/mg solid. Finally, FA release from the selected optimized supports was
36 studied following an *in vitro* digestion procedure. The results showed that amine-capped MSP
37 were not only able to hinder the release of the vitamin in gastric fluids (pH 2), but were also
38 capable of deliver progressively the FA in presence of a simulated intestinal juice (pH 7.5) offering
39 a suitable mechanism to control the bioaccessibility of the vitamin.

41 Keywords: Folic acid; bioaccessibility; loading optimization; controlled release; mesoporous silica
42 particles

43

44 **1. Introduction**

45

46 Folate is a generic term by which is known a group of water-soluble compounds with B9 vitamin
47 activity and with chemical structures similar to synthetic pteroyl monoglutamic acid (PGA),
48 commonly known as folic acid (FA). Folates are essential to numerous bodily functions, including
49 DNA synthesis and repair, cell division and cell growth [1]. Main folate sources include green leafy
50 vegetables, yeast extracts, liver, kidney, and citrus fruit. Despite this wide distribution, folate
51 deficiency is a common finding that can be caused by a variety of factors such as malabsorption of
52 folate from the diet, an increased utilization by the body or a significant loss up to 50% during
53 cooking processes [2]. FA deficiency is such important in humans that it can cause neural tube
54 defects in developing embryos [3], is associated with elevated plasma homocysteine (an emerging
55 risk factor for vascular diseases), with cognitive decline and neurodegenerative diseases such as
56 Alzheimer and also is risk factor for certain tumours (acute lymphoblastic leukaemia, breast
57 cancer, and gastric cancer) [4,5].

58

59 To prevent the occurrence of these and other diseases, food supplementation with folates is
60 mandatory in certain countries such as USA [6], Canada [7] or UK [8] with the objective of ensure
61 a 400 µg intake for adults and an additional 200 µg for pregnant women [9]. To achieve this
62 supplementation, the most employed molecule is FA, due to its high stability and bioavailability
63 [10].

64

65 Although there are irrefutable evidences about the benefits of FA supplementation to prevent
66 some diseases, recent studies suggest that the margin of the benefit is very narrow, and despite
67 the necessity of the supplementation, a massive exposition to high bioavailable FA could be a
68 double-edged sword [8]. In particular it has been reported that biotransformation processes of FA
69 are saturated at doses of 266-400 µg of FA and up to this amount unmetabolized FA is found in
70 plasma, which could be correlated with the increase of cancer risk, insulin resistance,
71 preneoplastic and neoplastic lesions [11]. In this context, the design of systems to dosage FA
72 along the digestion and therefore modulating its bioaccessibility and bioavailability is a challenge
73 for current nutritional science.

74

75 The bioaccessibility of a nutrient is defined as the amount of the nutrient that is released from a
76 food matrix during digestion and made accessible for absorption into the intestinal mucosa [12].
77 One possibility to modulate bioaccessibility of a molecule consists of its encapsulation and later
78 controlled release under suitable stimuli. Organic-based ensembles using lipids or carbohydrates
79 have been reported as classical encapsulation systems [13]. However, they have some important
80 drawbacks, such as the difficulty for a scale production [14, 15], low stability of the structure
81 during food processing and storage, difficulty of controlling the release rate and also a poor
82 capability to protect the encapsulated substance through the harsh stomach conditions [16]. As
83 an alternative, systems based in polyalcohols, polyamides, celluloses [17] or in mesoporous

84 inorganic materials [18], have been recently developed as suitable systems for controlled delivery
85 applications. In particular, mesoporous silica particles (MSP) exhibit unique features as supports
86 for controlled release, such as high stability [19], biocompatibility [20], no apparent toxicity [21],
87 large load capacity [22], and the possibility to include gate-like scaffoldings on the external
88 surface. This last characteristic allows the design of carriers for on-command delivery in the
89 presence of target physical (such as light, temperature) [23, 24], chemical (pH-changes, redox
90 potencial) [25-29] and biomolecules (enzymes, antibodies, DNA) [30-33] stimuli. Of those, several
91 gated MSP have proved to show “zero” delivery yet are able to release the cargo under digestive
92 stimuli [34, 35]. In particular, gated ensembles based in amines have been reported to be suitable
93 systems for cargo delivery upon pH changes.

94

95 The purpose of this study is, on one hand, to evaluate the use of MSP capped with amines as
96 suitable pH-responsive systems capable to modulate FA delivery and bioaccessibility in *in vitro*
97 digestion assays and on the other hand, to optimize the loading process in these materials to
98 achieve the release of the recommended dietary intake of folic acid using the minimum amount
99 of inorganic matrix. As far as we know, this is the first time that an optimization of folic acid
100 loading in MSP and a study of *in vitro* delivery from MSP of this molecule of nutritional interest is
101 reported.

102

103

104 **2. Materials and methods**

105

106 *2.1 Chemicals*

107 Tetraethylorthosilicate (TEOS), n-cetyltrimethylammonium bromide (CTABr), sodium hydroxide
108 (NaOH), triethanolamine (TEAH₃), the organosiloxane derivative 3-[2-(2-
109 aminoethylamino)ethylamino]propyl (N3), NaH₂PO₄, Na₂HPO₄ and Tetrabutylammonium
110 hydrogen Sulphate (TBAHS) and all chemicals for the digestive fluids were provided by Sigma-
111 Aldrich (Poole, Dorset, UK). Folic acid was purchased from Schircks Laboratories (Jona,
112 Switzerland). Acetonitrile HPLC grade was provided by Scharlau (Barcelona, Spain).

113

114 *2.2 FA molecular structural mechanics simulations*

115 Theoretical calculations of the structure of FA were carried out by using HyperChem 8.0.6 Molecular
116 Modeling System (Hypercube Inc., Gainesville, FL, USA). The calculation of geometry was performed using
117 molecular mechanics MM+ in a first step and AMBER in a second step. Full geometry optimizations were
118 carried out in vacuum employing the Polak-Ribiere conjugate gradient method until an RMS gradient of
119 0.1 kcal/mol was reached. The final 3D structure was refined by optimization of the geometry using
120 molecular dynamics methods at a simulation temperature of 300 K. QSAR properties of the vitamin were
121 determined.

122

123 *2.3 Synthesis of MCM-41*

124 The mesoporous MCM-41 support was first synthesized using the so-called “atrane route” in
125 which 4.68g of CTAB were added at 118°C to a solution of TEAH₃ (25.79 g) containing 0.045 mol of
126 a silatrane derivative (11 mL of TEOS). Next, 80 mL of water was slowly added with vigorous
127 stirring at 70 °C. After few minutes, a white suspension was formed. This mixture was aged at

128 room temperature overnight. The resulting powder was collected by filtration and washed with
129 water and ethanol. Finally, the solid was dried at 70 °C. To prepare the final mesoporous material,
130 the as-synthesized solid was calcined at 550 °C using an oxidant atmosphere for 5 h in order to
131 remove the template phase.

132

133 *2.4 Synthesis of **S0** and **S1***

134 100 mg of MCM-41 and 0.035 g (0.08 mmol) of FA were suspended in 7 mL of phosphate buffered
135 saline (PBS) inside an amber round-bottom flask in an inert atmosphere. The mixture was stirred
136 for 24h at room temperature to achieve the maximum loading in the pores of the MCM-41
137 scaffolding. The loaded solid (**S0**) was isolated by vacuum filtration, washed with 300 mL of water
138 adjusted to pH 2, and dried at room temperature for 24h. This loading process was optimized in
139 further assays (*vide infra* in 2.5).

140

141 To obtain **S1**, 100 mg of **S0** were suspended in 4 mL of acetonitrile and an excess of N3 (0.43 mL,
142 0.015 mmol) was added. The final mixture was stirred for 5.5 h at room temperature. The loaded
143 and functionalized solid (**S1**) was isolated by vacuum filtration, washed with 300 mL of water
144 adjusted to pH 2, and dried at room temperature for 24h.

145

146 *2.5 Folic acid release studies*

147 To determine the effect of pH in FA release from the non-gated (**S0**) and amine-gated (**S1**)
148 mesoporous silica particles, 10 mg of the corresponding solids (**S0** or **S1**) were placed in 25 mL of
149 water at pH 2 and pH 7.5. At a certain times aliquot were separated, the suspension filtered and
150 the solution analysed by HPLC.

151

152 *2.6 Folic acid loading optimization*

153 With the aim of optimize the amount of FA loaded inside the MSP, two different loading methods
154 were tested: immersion (A) and impregnation (B). Table 1 summarizes the 8 loading conditions
155 assayed. Solids were synthesized by triplicate.

156

157 For the immersion method (A), 100 mg of MCM-41 were immersed into a PBS solution containing
158 4 different amounts of FA, stirred for 24 h, filtered and washed. Then, loaded solids were
159 functionalized with 0.43 mL of N3 in acetonitrile following the procedure described in the
160 synthesis of **S1**. Using this method, 4 different loaded and functionalized solids were obtained
161 (**A1-4**).

162 For the impregnation method (B), FA dissolved in PBS (10mg/mL) was added to 100 mg of MCM-
 163 41 employing 4 different FA amounts and cycles of addition (see Table 1). After each addition
 164 cycle solids were dried at 30°C to eliminate water content. Then, each of the loaded solids (**B1-4**)
 165 were functionalized with 0.43 mL of N3 using different media; i.e. water at pH 2 (solids **BW#**),
 166 acetate buffer at pH 2 (**BB#** solids) or acetonitrile (**BA#** solids). The loaded and functionalized
 167 solids were isolated by vacuum filtration, washed with 300 mL of water adjusted to pH 2 with HCl,
 168 and dried at room temperature for 24h. Finally, 12 solids were obtained: 4 functionalized in water
 169 at pH 2 with HCl (**BW1-4**), 4 functionalized in acetate buffer at pH2 (**BB1-4**) and 4 functionalized in
 170 acetonitrile (**BA1-4**).

171

172 **Table 1.** Conditions employed in loading optimization assays: immersion method (A) and
 173 impregnation method (B).

174

<i>Loading mechanism</i>	<i>Solid</i>	<i>MCM (mg)</i>	<i>Folic (mg)</i>	<i>PBS (mL)</i>	<i>C_{folic} (mg/mL)</i>	<i>Cycles (amount of solution per cycle)</i>
<i>Immersion</i>	A1	100	35	7	5	
	A2	100	35	3.5	10	
	A3	100	70	7	10	
	A4	100	70	3.5	20	
<i>Impregnation</i>	B1	100	10	1	10	1 (1 mL)
	B2	100	10	1	10	2 (0.5 mL)
	B3	100	15	1.5	10	3 (0.5 mL)
	B4	100	20	2	10	4 (0.5 mL)

175

176

177 2.7 Loading efficiency evaluation

178 Loading efficiency of each of the 16 obtained solids was determined by quantification FA
 179 delivered in PBS after 5h by HPLC. The “relative loading efficiency” was calculated according to
 180 the following equation:

181

$$182 \text{ Relative loading efficiency (\%)} = \text{FA}_D / \text{FA}_L \times 100$$

183

184 where FA_D are the mg of folic delivered per 1mg of loaded solid and FA_L are the mg of folic acid
 185 employed for the loading of 1 mg of MCM-41.

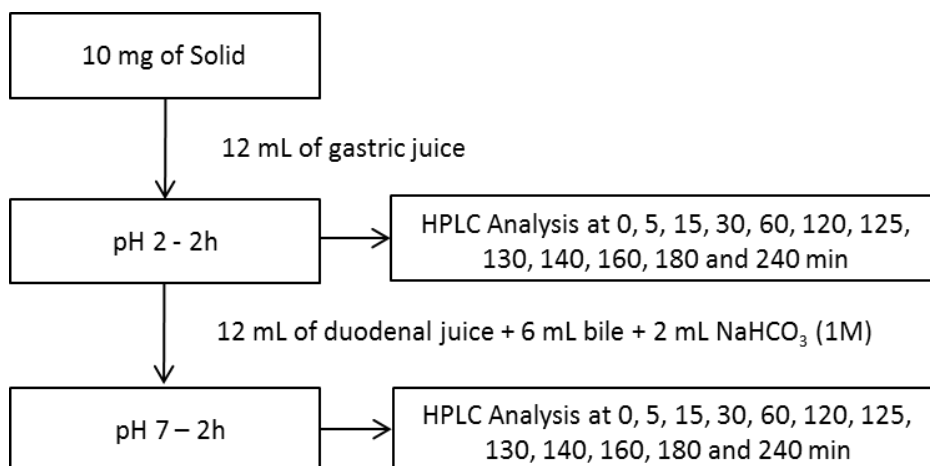
186

187 2.8 Determination of *in vitro* folic acid bioaccessibility

188 FA bioaccessibility (FA delivery from the prepared solids) was determined by simulating a human
 189 digestion in the stomach and small intestine adapting the procedure described by Versantvoort et
 190 al. [36] (Fig. 1). The large intestinal track was not taken into account since *in vivo* folic acid
 191 absorption occurs throughout the jejunum [1]. In a typical experiment, 10 mg of the
 192 corresponding solid were suspended in 12 mL of gastric juice and incubated for 2h at 37°C.
 193 Finally, 12 mL of duodenal juice, 6 mL of bile, and 2 mL of bicarbonate solution (1M) were added
 194 simultaneously. After the addition, the mixture was maintained under stirring at 37°C for 2h. All

195 digestive juices were heated to 37°C before being mixed. During this period aliquots were taken,
 196 filtered and analysed by HPLC.

197



198

199

Figure 1. Schematic representation of the *in vitro* digestion model.

200

201 2.9 Folic acid determinations

202 FA was determined by reversed-phase gradient HPLC method according to the method described
 203 by Póo-Prieto et al. [37] with minor modifications. The HPLC instrument consisted of a Hitachi
 204 LaChrom Elite liquid chromatograph (Hitachi Ltd., Tokyo, Japan) equipped with an auto-sampler
 205 and UV detector (model L-2400). A Kromaphase 100 C18 (250 mm x 4.6 mm i.d., 5 µm particle size
 206 analytical column) (Scharlab, Barcelona, Spain) was used for the separations. Mobile phase
 207 consisted of (A) 0.125 mM of NaH₂PO₄, 0.875 mM of Na₂HPO₄ and 0.4mM of TBAHS in water and
 208 (B) acetonitrile-phase A 65:35 (v/v). The flow rate employed is described in table 2. The
 209 wavelength of UV detector was set at 280 nm. Solutions for preparation of calibration standards
 210 were made at 1, 5, 10, 25, 50, 75, 100 µg FA/mL in PBS.

211

212

Table 2. Elution program for HPLC analysis.

Time (min)	Flow (mL/min)	Mobile phase A (%)	Mobile phase B (%)
0	1.0	90	10
5	1.0	90	10
15	1.0	64	36
30	1.0	40	60
35	1.0	90	10
40	1.0	90	10

213

214 A: NaH₂PO₄ (0.125 mM), Na₂HPO₄ (0.875 mM) and TBAHS (0.4mM) in water.

215 B: Acetonitrile-Phase A 65:35 (v/v)

216

217 **2.10 Solids characterization**

218 X-ray diffraction (XRD), transmission electron microscopy (TEM), N₂ adsorption-desorption
219 isothermes and thermogravimetric analyses (TGA) were employed to characterize the synthesized
220 materials. XRD were performed on a BrukerD8 Advance diffractometer using CuK α radiation. TEM
221 images were obtained with a JEOL JEM-1010. The N₂ adsorption-desorption isotherms were
222 recorded by a Micrometrics ASAP2010 automated sorption analyser. Samples were degassed at
223 90°C in vacuum, overnight. The specific surface areas were calculated from the adsorption data
224 within the low pressure range using the BET model. Pore size was determined following the BJH
225 method. Thermogravimetric analyses were carried out on a TGA/SDTA 851e Mettler Toledo
226 balance, using an oxidant atmosphere (air, 80 mL/min) with a heating program consisting of a
227 heating ramp of 10 °C per minute from 393 to 1273 K and an isothermal heating step at this
228 temperature for 30 min.

229

230

231 **2.11 Data analysis**

232 The results of the FA delivery from the different solids prepared were statistically processed using
233 Statgraphics Centurion XV (Manugistics Inc., Rockville, MD, USA). Statistical analysis on FA
234 concentrations was made using an analysis of variance (One-Way ANOVA).

235

236 **3. Results and discussion**

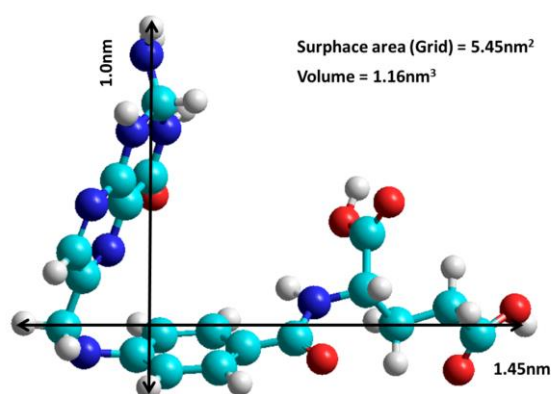
237

238 **3.1 FA molecular modelling and geometrical dimensions**

239

240 Molecular dynamics calculations on FA were carried out. The molecular structure of FA is shown
241 in Figure 2. As it can be seen, FA (pteroyl monoglutamic acid) consists of a pteridin ring linked to
242 the para-amino benzoic acid (PABA) and a molecule of glutamic acid. In the larger dimension, FA
243 exhibits a length of 1.45 nm, whereas the calculated volume is 1.16 nm³. These calculations were
244 used to determine the total theoretical amount of vitamin that could be encapsulated in the silica
245 mesoporous matrix (vide infra).

246



247

248 **Figure 2.** 3D FA molecular structure and geometrical dimensions

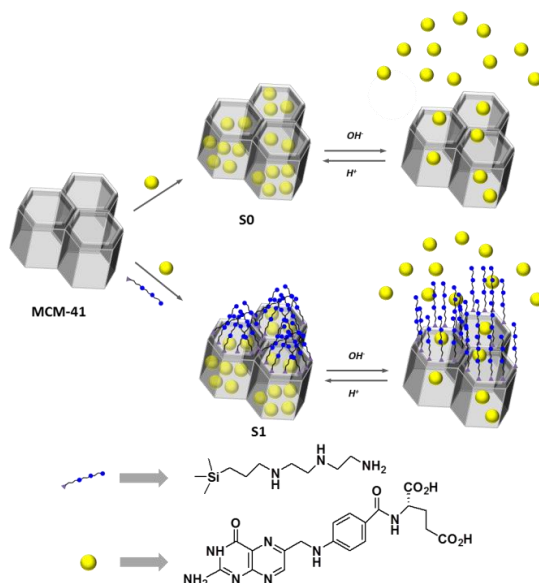
249

250 3.2 Design, synthesis and characterization of the gated particles

251 For the design of the proposed pH-controlled and sustained release system described above
252 MCM-41 mesoporous silica microparticles were selected as an inorganic support due to its high
253 loading capacity, homogeneous porosity in the 2–3 nm range, high inertness, and ease of
254 functionalization. This starting support was loaded with FA to obtain solid **S0**. Moreover, this FA-
255 loaded material was further capped with a pH-responsive ensemble (i.e. 3-[2-(2-
256 aminoethylamino)ethylamino]propyltrimethoxysilane, N3) in order to obtain the gated
257 polyamine-functionalised material **S1**. In this work pH was chosen as a suitable digestive stimulus
258 for the modulation of FA release from the inner of the MCM-41 voids. In stomach, pH is very acid
259 (pH 1-2) to help the degradation of proteins and to provide a non-specific immunity, retarding or
260 eliminating various pathogens. In the small intestine, the duodenum provides critical pH balancing
261 to activate digestive enzymes. The liver secretes bile into the duodenum to neutralise (pH 7-7.5)
262 the acidic conditions from the stomach. Also the pancreatic duct empties into the duodenum,
263 adding bicarbonate to neutralize the acidic chyme, thus creating a neutral environment. FA is
264 known to be mainly absorbed in the small intestine (jejunum; pH 7.5) from where it is distributed
265 to the tissues through the bloodstream and stored in the liver.

266

267 As stated above, pH has been chosen in this paper as triggering stimulus. In this particular system
268 changes in the pH are expected to modulate FA delivery in two different ways. On the one hand, it
269 is known that FA under neutral/basic conditions is about 1000 times more soluble than FA in an
270 acidic environment due to protonation (acid) and deprotonation (neutral/basic) of FA in aqueous
271 environments [38]. On the other hand, it has been reported that MSP functionalised with the
272 polyamine derivative 3-[2-(2-aminoethylamino)ethylamino]propyl-trimethoxysilane (N3) are
273 suitable pH-responsive controlled release systems able to allow or inhibit delivery as a function of
274 pH changes due to the transformation of amines (open gate at neutral/basic pH) to
275 polyammonium groups (closed gate at acidic pH). These two mechanisms of action are illustrated
276 in Figure 3.



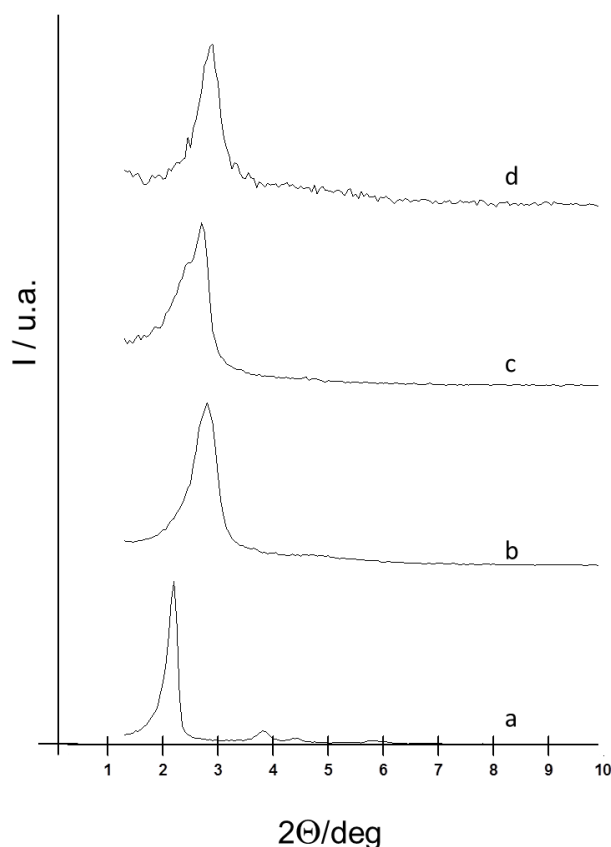
277

278 **Figure 3.** Illustration of the synthetic procedure for the preparation of solids **S0** and **S1**, and the
279 mechanism of FA delivery at neutral or acidic conditions.

280

281 The different solids prepared were characterized according to standard techniques. X-ray patterns
282 of the solids MCM-41 as synthesized (*a*), calcined (*b*), loaded with folic acid (**S0**) (*c*) and loaded
283 with folic acid and functionalized with amines (**S1**) (*d*) are shown in Figure 4. Curve *a* shows the
284 expected four peaks of a hexagonal ordered array indexed as (100), (110), (200) and (210) Bragg
285 reflections. A significant shift of the (100) reflection in the XRD powder of the MCM-41 calcined
286 sample is clearly appreciated in the curve *b*, corresponding to a cell contraction related to
287 condensation of silanols during the calcination step. Curves *c* and *d* show that reflections (110),
288 (200) and (210) are lost, most likely due to a reduced contrast that can be attributed to the
289 presence of FA in the pore voids and the anchored N3 molecule. Nevertheless, the existence in all
290 cases of the (100) peak in the XRD patterns indicated that the process of pore loading with FA,
291 and the additional functionalization with the polyamine, did not modify the typical porosity of the
292 mesoporous MCM-41 scaffold.

293



294

295 **Figure 4.** Powder X-ray patterns of the solids (a) MCM-41 as-synthesized, (b) MCM-41 calcined, (c)
296 the uncapped solids containing the vitamin B₉ (**S0**) and (d) the capped mesoporous system (**S1**).

297

298 The MCM-41 mesostructure after loading with FA and functionalization with
299 polyamines was also confirmed by TEM images (see Figure 5).

300

301

302

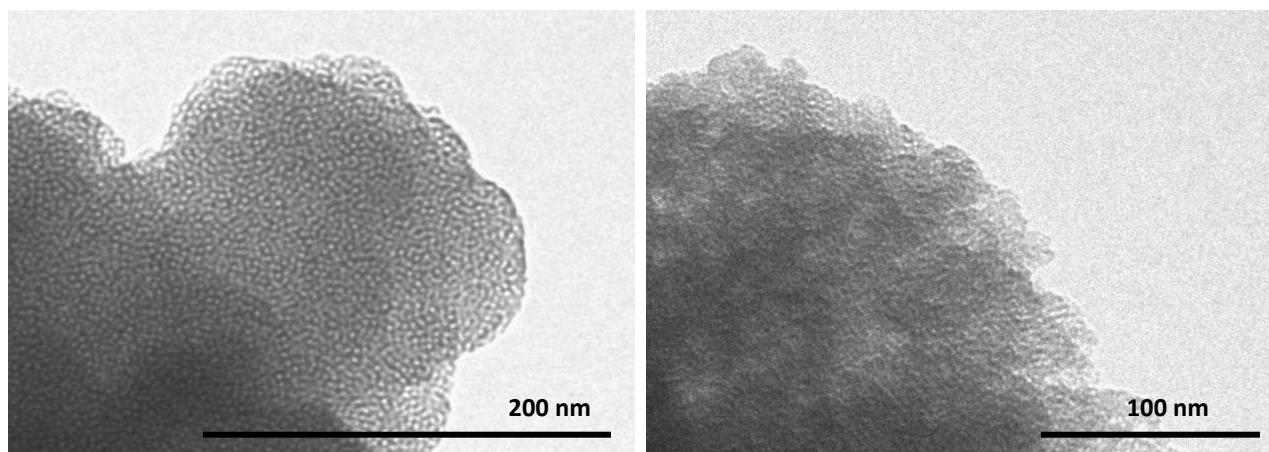


Figure 5. TEM image of (a) MCM-41 calcined and (b) solid **S1** showing the typical porosity of the MCM-41 matrix.

The N_2 adsorption-desorption isotherms of the starting MCM-41 calcined material are shown in Figure 6. The curve shows a well defined and sharp adsorption step at P/P_0 values between 0.1 and 0.3, corresponding to a type IV isotherm, which is typical of mesoporous materials, attributed to nitrogen condensation in the mesopore inlets. With the Barrett-Joyner-Halenda (BJH) model on the adsorption curve of the isotherm, pore diameter and pore volume were calculated to be 2.52 nm and $0.92 \text{ cm}^3 \text{ g}^{-1}$, respectively. The absence of a hysteresis loop in this interval and the narrow BJH pore distribution suggested the existence of uniform cylindrical mesopores. The application of the BET model resulted in a value of $1040 \text{ m}^2/\text{g}$ for the total specific surface. From the XRD, porosimetry and TEM studies, the a_0 cell parameter (3.98 nm), the pore diameter (2.52 nm), and a value for the wall thickness of 1.69 nm were calculated.

Considering the pore size of the MCM-41 support and the FA structure (see section 3.1), it can be stated that FA can be perfectly encapsulated in pores of 2.52 nm of diameter. Moreover, bearing in mind the volume of the FA molecule (1.16 nm^3), the specific volume of the MCM-41 ($0.92 \text{ cm}^3/\text{g}$) and tentatively assuming that ca. 75% of the pore volume in the mesoporous support can be occupied by FA, it can be roughly established that 1 mg of MCM-41 could host as a maximum 436 μg (0.98 mmol) of FA in its porous network.

Table 3 also shows the change on the textural properties of the starting silica after the vitamin adsorption (**S0**) and the functionalization with the N3 molecule (**S1**). The incorporation of the FA leads to a decrease of ca. 37% and 46% for the BET surface area and the BJH mesopore volume, respectively. This evolution indicates that the FA molecules must be incorporated inside the mesopores. Under the pH conditions used for the drug uptake (7.5), the two carboxylate groups must be deprotonated, and consequently, the interaction with the silanol groups at the silica surface must be mediated by H^+ species. Taking into account the presence of partially filled mesopores in the solid **S0** together with the relatively large arm of the N3 molecule, the incorporation of these last species preferentially must occur in the external surface at the mesopore entrances. As expected, the incorporation of the N3-gates leads to an additional decrease of both the surface area as the volume of 31 and 57%, respectively. In a parallel way,

346 the size of the mesopores decreases after FA inclusion. A large variety of FA aggregates on the
 347 silica are possible which is consistent with the wider peak observed in the pore size distribution
 348 curve. An additional mesopore size reduction occurs after functionalization with N3 groups.
 349 Hence, solid **S1** shows a wide pore size distribution with a principal peak centred at 1.82 nm and a
 350 residual signal at ca. 2.38 nm. The first peak could be associated to a majority of the mesopores
 351 well surrounded by N3 molecules and the residual peak must be attributed to a small proportion
 352 of mesopores showing some deficiencies respect to an optimum presence of N3 groups.

353

354

355

356 **Table 3.** Analytical and textural parameters from TGA and N2 adsorption-desorption isotherms.

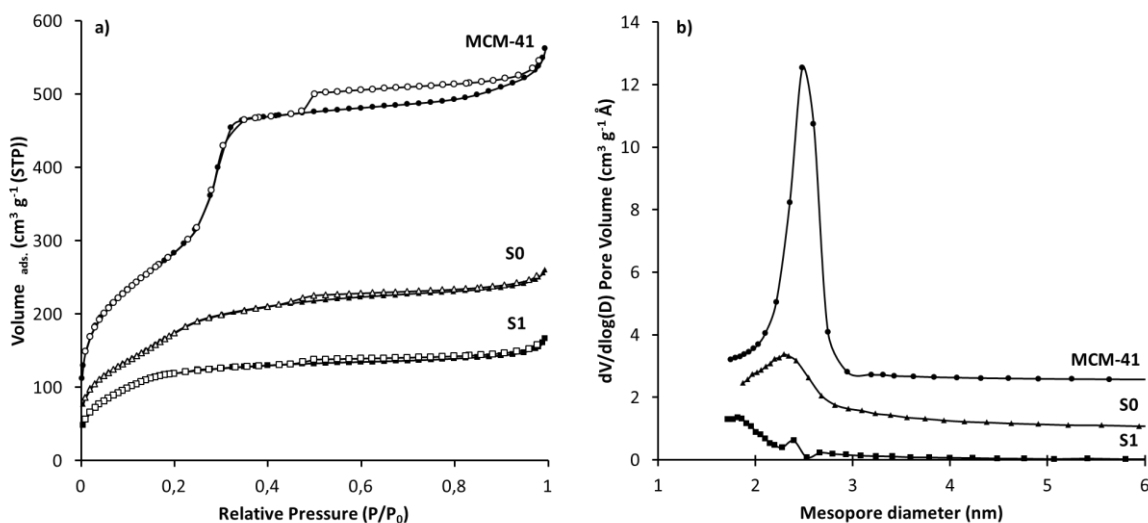
357

	SBET (m ² g ⁻¹)	Pore volume (cm ³ g ⁻¹)	Pore size (nm)
MCM-41	1040	0.92	2.52
S0	653	0.49	2.28
S1	451	0.21	1.82 (2.38)

358

359

360



361

362 **Figure 6.** Nitrogen adsorption-desorption isotherms (a) and pore size distribution (b) for MCM-41
 363 mesoporous material, S0, and S1 materials.

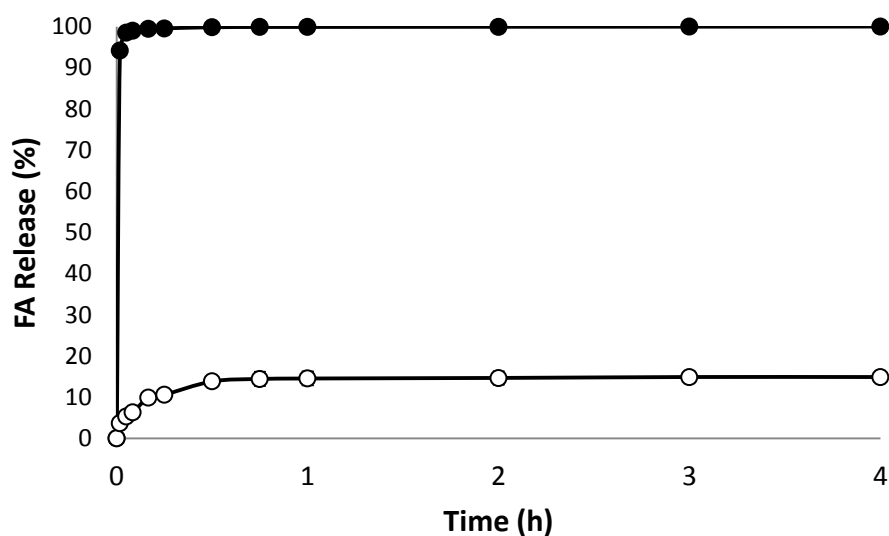
364

365

366 3.3 pH gate-like mechanism confirmation

367 FA delivery from the uncapped solid **S0** in acid and neutral conditions was studied. In a typical
 368 experiment 5 mg of **S0** were suspended in 25 mL of two different aqueous solutions (pH 2 and pH
 369 7.5) in an attempt to reproduce the pH of gastric or intestinal fluids. The release profile of **S0** is
 370 shown in Figure 7.

371



373

374

Figure 7. Release profiles of folic acid from the pores of solid **S0** in water at pH 2 (unfilled marker points) and pH 7.5 (filled marker points). Values are Means \pm SD, n=3.

375

376

377

378

379

380

381

382

383

384

385

386

387

388

389

390

391

392

393

394

395

396

397

398

399

400

401

As observed in the Figure 7, the asymptote of the release curve was achieved in the first few minutes of the delivery at pH 7.5. According to TGA experiments, the maximum delivery achieved (indicated in the figure as 100%) corresponds to 32% of the FA content in the solid. This indicated that, under the experimental conditions, not all the FA loaded was able to be released. In contrast, only a $14.9\pm 1.2\%$ of the maximum delivery capacity was achieved at pH 2 (which corresponds to ca. 5% of the total FA content determined by TGA). Considering that the increase of FA concentration in the water phase is proportional to the delivery of the vitamin from the pores and that FA release is not inhibited by the presence of functional molecular groups on the surface of the MCM-41, the effect of solubility in FA bioaccessibility (release) is confirmed. At pH 2, FA is in the form of acid with low solubility, while at pH 7.5 folic is in the form of salt, increasing its solubility, and enhancing the delivery [39] from the pore voids of **S0** to the solution. However, as it can be seen in figure 7 this pH-induced “solubilisation mechanism” is insufficient to modulate a sustained release of FA, a fact that would not allow a proper absorption of FA in the jejunum.

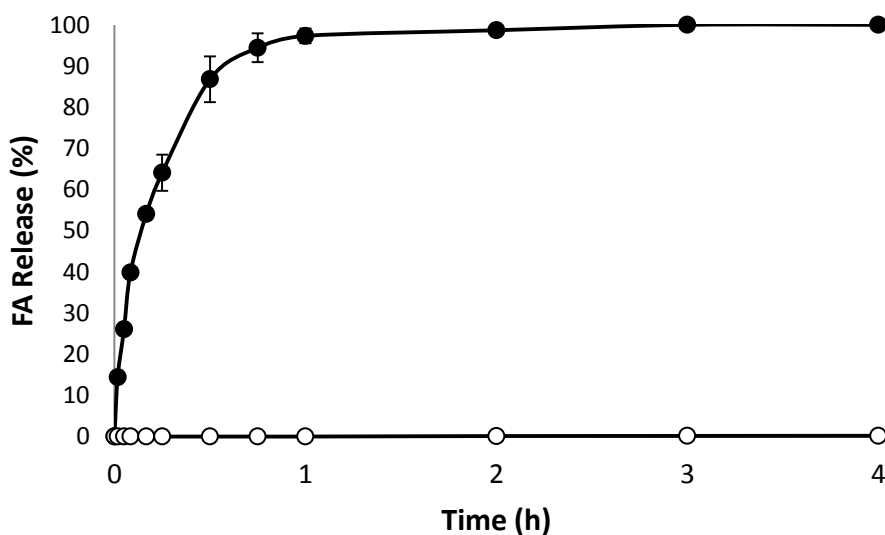
In a second study, delivery of FA from **S1** was tested using similar delivery conditions; i.e. 5 mg of **S1** were suspended in 25 mL of two different aqueous solutions at pH 2 and pH 7.5. As shown in Figure 8, FA delivery after 4h at pH 2 achieved values $0.22\pm 0.03\%$ of the maximum delivery capacity of **S1** (which corresponds to ca. 0.09% of the total FA content determined by TGA). In contrast, at pH 7.5, a progressive delivery of the vitamin was observed, achieving ca. 100% of the release capacity in the performed conditions after 1h (which corresponds to 40% of FA content determined by TGA). In this case, the pH-dependent release behaviour can be explained by considering the different FA solubility as a function of the pH and the presence of the gate-like ensemble based in polyamines. To explain this latter effect, it has to be taken into account that at acidic conditions (pH 2), amines anchored to the surface of the pores are fully protonated. This

402 fact favours Coulombic repulsions between closely located polyammonium groups, so that
403 tethered polyamines tend to adopt a rigid-like conformation that blocks the pores and practically
404 no release occurs. At pH 7.5, a lower proportion of polyamines are expected to be protonated,
405 favouring hydrogen bond interactions between the different amine chains. As a consequence,
406 pores unblock and vitamin release is produced. Moreover, in amine-based gated ensembles a
407 second cooperative anion-dependent effect occurs. In general polyamines are well-known pH-
408 responsive molecules that can additionally complex anions via electrostatic forces and by
409 formation of hydrogen-bonding interactions in a wide pH range. Additionally, the relative
410 amine/ammonium ratio can control the interaction with anionic species. If electrostatic forces are
411 taken into account (which in general are stronger than hydrogen bonding interactions) the
412 presence of a large percentage of ammonium groups (acidic pH) will favour the interactions of the
413 “gate” with anions in the solution resulting in an additional pore blockage that is not observed at
414 neutral or basic pH [40].

415

416 Comparing the delivery profiles at pH 2 and 7.5 of the uncapped (**S0**) and capped (**S1**) materials it
417 is apparent that **S0** is not able to completely inhibit FA delivery at acidic pH being the delivery very
418 fast at neutral pH. In contrast, **S1** is tightly capped at pH 2 and displays a sustained delivery (in 1h)
419 when the pH is switch to 7.5. It can be concluded that the gated support **S1** might be a suitable
420 prototype for the development of orally applicable FA delivery systems designed to block cargo
421 delivery in the acidic conditions of the stomach (acid pH, gate closed) yet be able to display a
422 sustained FA release at the intestine (basic pH, gate open).

423



424

425 **Figure 8.** Release profiles of folic acid from the pores of solid **S1** in water at pH 2 (unfilled marker
426 points) and pH 7.5 (filled marker points). Values are Means \pm SD, n=3

427

428 3.3 Loading/releasing optimization process

429

430 After studying the delivery of FA from the polyamine-functionalised (**S1**) and unfunctionalised (**S0**)
431 materials, this section deals with a detailed study of FA loading optimization for the preparation
432 of functionalised solids (**S1**-like supports). For this purpose, 16 solids differing in the loading
433 (immersion and impregnation) and the functionalization media used to anchor the polyamine N3
434 (water at pH 2, acetate buffer at pH 2 or acetonitrile) were prepared. Delivery effectiveness of
435 each solid was evaluated by the determination of FA delivered after 5h at pH 7.5. Moreover, the
436 loading/delivery performance of the solids was evaluated using the “relative loading efficiency”
437 via the determination of the ratio between the amount of FA delivered (after 5h at pH 7.5) per mg
438 of loaded solid and the mg of FA used for loading 1 mg of MCM-41 (see Experimental Section for
439 details).

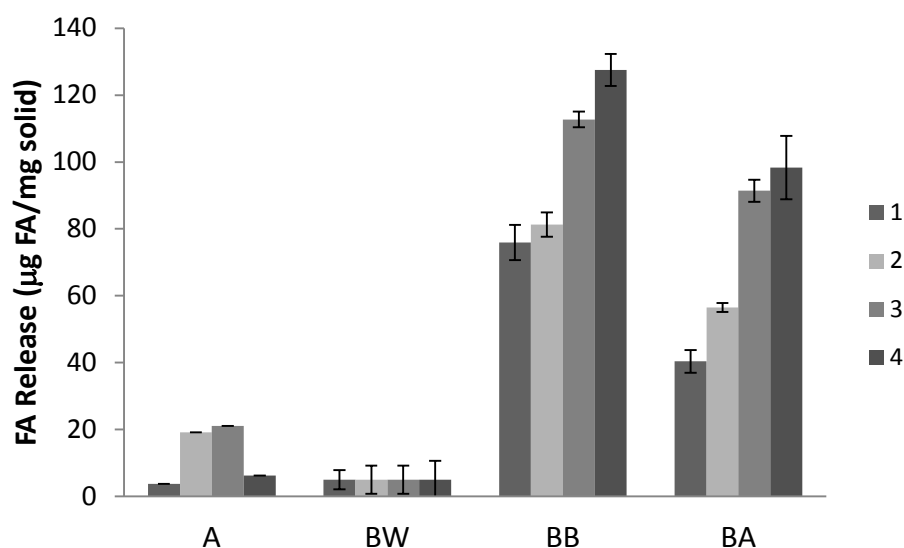
440

441 The first block of bars of Figure 9 shows values of FA delivered per mg of **A#** solids, solids obtained
442 by using a traditional immersion procedure. Among them, solid **A1** was able to deliver $3.7 \pm 0.2 \mu\text{g}$
443 of FA/mg of solid. By increasing the amount of FA present in the loading solution to 70mg
444 (0.016mmol) (**A3**) the amount delivered increased to $21.2 \pm 0.3 \mu\text{g}$ of FA/mg of solid. However,
445 when the same amount of folic was loaded in the half of solvent, the release capacity decreased
446 (**A4**) to $6.2 \pm 0.2 \mu\text{g}$ of FA/mg of solid. To understand this behaviour the maximum FA amount able
447 to be solubilized in PBS was determined, finding that above of 10mg of FA/mL PBS, FA remains
448 insolubilized, and thus, cannot participate in the loading process.

449

450 The same figure shows values of FA delivered by solids loaded by impregnation and functionalized
451 in water at pH 2 (**BW#**), acetate buffer at pH 2 (**BB#**) or acetonitrile (**BA#**). As it can be seen, **BW#**
452 solids exhibited the lowest loading capacity. In fact the 4 solids prepared using these conditions
453 were white, strongly suggesting the presence of a very low amount of FA (pale yellow) in the
454 pores. To understand the cause of this behaviour, it was found that pH reached values of 10 upon
455 the addition of the amine N3 during the synthesis of the solid. At this pH FA is highly soluble and
456 most likely leaked from the pore voids during the synthesis of the materials. In contrast, **B** solids
457 functionalized with N3 in aqueous acetate buffer (**BB#** solids) or acetonitrile (**BA#** solids), showed
458 a remarkable larger FA delivery in water. In this case, the poor solubility of FA in the acetate
459 buffer or acetonitrile during the N3 functionalization avoided the FA leakage during this step of
460 the synthesis. When both **BA#** and **BB#** solids are compared in terms of delivery, it can be stated
461 the **BB#** series display larger delivery ability. In particular, **BB#** solids exhibited a remarkable
462 delivery capacity ($p < 0.005$), being solid **BB4** able to release $127 \pm 5 \mu\text{g}$ of FA/mg of solid (see Figure
463 9). As a conclusion, the choice of the solvent employed for the surface functionalization step is as
464 important as the loading procedure in terms of loading efficiency. Nevertheless, the maximum
465 loading capacity calculated in section 3.2 has not been achieved in any of the designed solids.

466

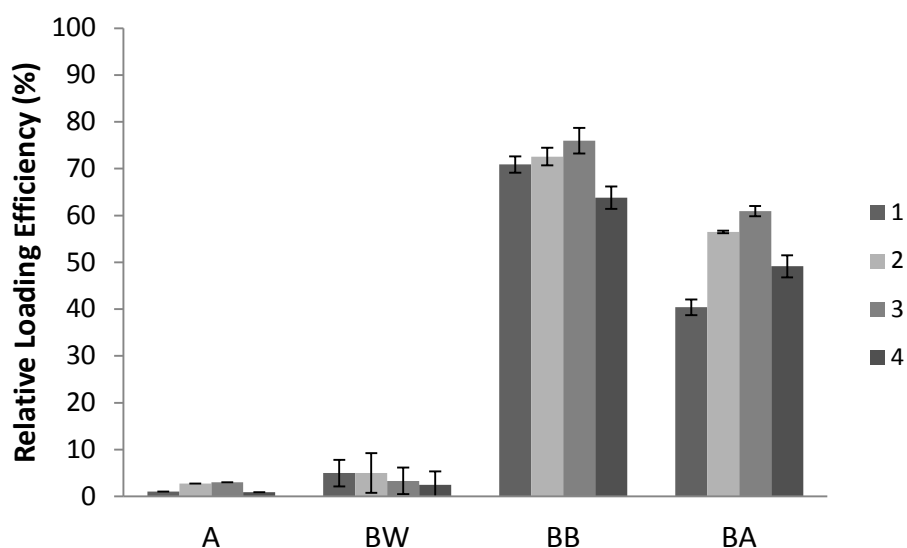


467
 468 **Figure 9.** Maximum FA delivery ($\mu\text{g FA/mg solid}$) for different solids loaded by immersion in PBS
 469 and functionalized with N3 in acetonitrile (A# solids) or loaded by impregnation and
 470 functionalized with N3 in different solvents: water adjusted to pH 2 (BW), acetate buffer at pH 2
 471 (BB) or acetonitrile (BA). Numbers 1-4 refers to different FA loading conditions described in Table
 472 1. Values are Means \pm SD, n=3.

473
 474 From the release ability displayed by the different solids prepared and taking into account the
 475 amount of FA employed for the loading of each solid, the relative loading efficiency (RLE) was
 476 calculated. Figure 10 shows RLE values for the 16 prepared solids. As expected, solids loaded by
 477 immersion (A#) were the less efficient in terms of delivery with RLE values of around 1-3%.
 478 Moreover RLE values of ca. 2.5-5%, 40-60% and 63-75% were observed for BW#, BA# and BB#
 479 supports. In addition, for solids BA# and BB# RLE increased significantly ($p < 0.005$) from 10 mg in 1
 480 cycle (#1 solids) to 15 mg in 3 cycles (#3 solids). However, the addition of 1 extra cycle of addition
 481 (#4 solids) did not increase RLE values indicating that, in this case, not all the FA added was loaded
 482 inside the pore voids of the mesoporous materials. According to these results, the conditions
 483 employed for preparing solid BB3 should be considered as optimal, in terms of RLE values, for the
 484 preparation of MSP loaded with folic acid and gated with N3 moieties.

485
 486 All these prepared solids were characterized using standard techniques. In all cases XRD patterns
 487 and TEM images (data not shown) were equivalent to those obtained for solid S1 (section 3.1),
 488 confirming that the mesoporous structure of the MCM-41 scaffold was maintained in spite of the
 489 different loading and functionalization process.

490
 491



492
 493 **Figure 10.** Relative Loading Efficiency for different solids loaded by immersion in PBS and
 494 functionalized with N3 in acetonitrile (A# solids) or loaded by impregnation and functionalized
 495 with N3 in different solvents: water adjusted to pH 2 (BW# solids), acetate buffer at pH 2 (BB#
 496 solids) or acetonitrile (BA# solids). Numbers 1-4 refers to different FA loading conditions described
 497 in Table 1. Values are Means±SD, n=3.

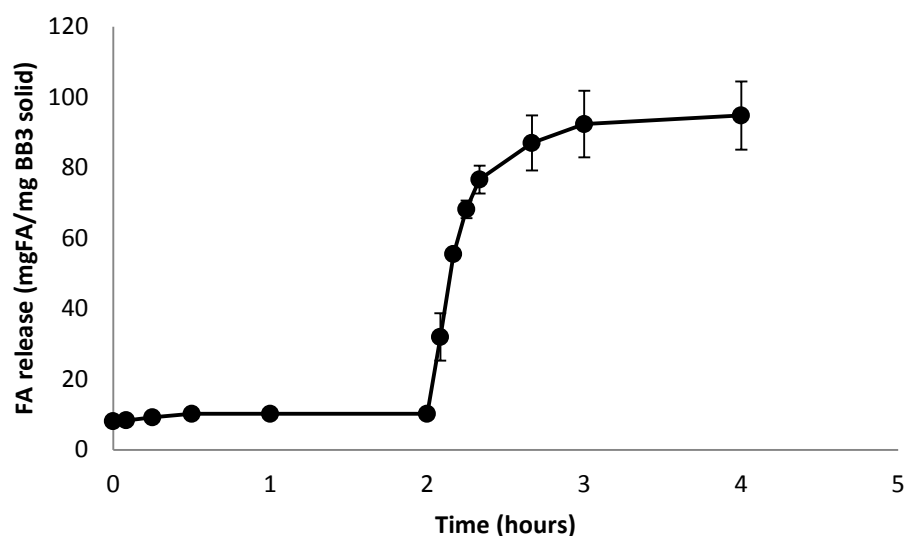
498

499 3.4 *In vitro* Folic Acid bioaccessibility and nutritional implications

500

501 After the loading optimization procedure described above, this section deals with the use of solid
 502 **BB3**, which exhibited the maximum RLE value, for delivery studies in a more realistic media. In
 503 particular, the aim of this part was to study FA release, and therefore FA bioaccessibility, during a
 504 simulated pass of the solid through the gastrointestinal tract. To evaluate this, a variation of the
 505 dynamic *in vitro* digestion protocol reported by Versantvoort et al. [36] was performed. Briefly
 506 **BB3** was suspended in simulated gastric juice and incubated for 2h at 37°C and then duodenal
 507 juice, bile and bicarbonate solution were added to obtain a simulated intestinal fluid (see
 508 Experimental Section for details). Note that in this study the pass of the solid through large
 509 intestinal track was not taken into account since *in vivo* folic acid absorption occurs throughout
 510 the jejunum [1]. At certain times aliquots were taken, filtered and analysed by HPLC. Results of FA
 511 delivery from **BB3** are shown in Figure 11. During the first two hours of simulated digestion,
 512 where **BB3** solid was in contact with a simulated gastric fluid, only 10.2±1.4 µg of FA/mg of solid
 513 were delivered. After the addition of the simulated intestinal fluid, FA delivered increased
 514 progressively to reach a maximum value of 94±9 µg of FA/mg of solid at 2h.

515



516
 517 **Figure 11.** Release profile of FA from solid BB3 along the simulated gastrointestinal digestion
 518 process. Time 0-2h correspond to the simulation of stomach conditions and time from 2-4h
 519 correspond with the simulation of intestinal conditions. Values are Means±SD, n=3.
 520

521 Thus, as it can be observed in Figure 9, **BB3** solid is tightly capped in simulated gastric fluid yet
 522 opens and deliver the cargo when in contact with simulated intestinal fluid. Moreover, the most
 523 important thing is that 1 mg of solid **BB3** is able to release ca. 95 µg of FA during the whole
 524 simulated digestion process. This implicates that the higher recommended dietary intakes in
 525 human nutrition, established for pregnant woman in 600 µg per day of folates or 360 µg of
 526 synthetic PGA (1 µg of dietary folate equivalent = 0.6 µg of folic acid) [9, 41], could be reached by
 527 an oral administration of only ca. 4 mg of **BB3**, which is a remarkable low amount. Moreover,
 528 based in the oral toxicological evaluation of other mesoporous silica particles carried out by
 529 Kupferschmidt et al. [42] -that found that even high amounts of MSP up to 1200 mg of MSP/kg of
 530 rat administrated orally were not toxic - our less than 7 mg are very far of a toxicological effect,
 531 signifying that the optimized solid **BB3** could be safe for oral administration.

532

533

534 4. Conclusions

535

536 Mesoporous silica particles (MSP) have been recently proposed as smart delivery devices able to
 537 load large amounts of cargo and release the same using different triggering stimuli. In this study
 538 FA has been successfully encapsulated in mesoporous silica particles capped with 3-[2-(2-
 539 aminoethylamino)ethylamino]propyl groups. A detailed study of the loading process allowed us to
 540 obtain solids with relative encapsulation efficiencies of the 75%. The simulation of an *in vitro*
 541 digestion of selected optimized gated support allowed to conclude that the developed MSP
 542 capped with amines were not only able to hinder the release of the vitamin in the presence of a
 543 simulated gastric fluid, but also were able to deliver progressively the vitamin along the time in
 544 presence of a simulated intestinal fluid, offering a mechanism to modulate the bioaccessibility of

545 the FA vitamin during the pass across the intestine. In this study it was found that 1 mg of the
546 optimized solid was able to release ca. 95 µg of FA indicating that maximum levels of higher
547 recommended dietary intakes in human nutrition could be reached using only 4 mg of the
548 optimized solid. Bearing additionally into account that mesoporous silica particles are non-toxic at
549 low levels for humans, it can be stated that pH-dependent capped SMP are suitable candidates for
550 the design of orally applicable delivery systems designed to protect FA from the acidic conditions
551 of the stomach (acid pH, gate closed) but release the vitamin at the intestine (basic pH, gate
552 open).

553

554

555 **Acknowledgements**

556 Authors gratefully acknowledge the financial support from the Ministerio de Economía y
557 Competitividad (Projects AGL2012-39597-C02 and MAT2012-38429-C04-01) and the Generalitat
558 Valenciana (project PROMETEO/2009/016). E.P. is grateful to the Ministerio de Ciencia e
559 Innovación for his grant (AP2008-00620).

560

561 **References**

562

563 [1] M. Lucock, *Mol. Genet. Metab.* 71 (2000) 121-138

564 [2] I.R. Younis, M.K Stamatakis, P.S. Callery, P.J. Meyer-Stout, *Int. J. Pharm.* 367 (2009) 97-102

565 [3] A.E. Czeizel, I. Dudás, *New Engl. J. Med.* 327 (1992) 1832-1835

566 [4] A.J.A. Wright, P.M. Finglas, S. Southon, *Trends Food Sci. Tech.* 12 (2001) 313-321

567 [5] H. Koike, T. Hama, Y. Kawagashira, R. Hashimoto, M. Tomita, M. Iijima, G. Sobue, *Nutrition* 28
568 (2012) 821-824

569 [6] Food and Drug Administration, *Fed Regist.* 61 (1996) 8752-8807

570 [7] Health Canada, *Can. Gaz.* 131 (1997) 8752-8807

571 [8] M. Lucock, Z. Yates, *Curr. Opin. Clin. Nutr. Metab. Care* 12 (2009) 555-564

572 [9] M. Eichholzer, O. Tönz, R. Zimmermann, *Lancet* 367 (2006) 1352-1361

573 [10] P. Sanderson, H. McNulty, P. Mastroiacovo, I.F. McDowell, A. Melse-Boonstra, P.M. Finglas,
574 J.F. Gregory *Brit. J. Nutr.* 90 (2003) 473-479

575 [11] Y.I. Kim, *Environ. Mol. Mutagen.* 44 (2004) 10-25

576 [12] E. Hedrén, V. Diaz, U. Svanberg, *Eur. J. Clin. Nutr.* 56 (2002) 425-430

577 [13] S. Tomiuk, Y. Liu, T.J. Green, M.J. King, P.M. Finglas, D.D. Kitts, *Food Chem.* 133 (2012) 249-
578 255

- 579 [14] L. Chen, G.E. Remondetto, M. Subirade, Trends Food Sci. Tech. 17 (2006) 272–283
- 580 [15] M. Fathi, M.R. Mozafari, M. Mohebbi, Trends Food Sci. Tech. 23 (2012) 13–27
- 581 [16] D.J. McClemens, Y. Li, Food Funct. 1 (2010) 32-59
- 582 [17] M. Mastromatteo, M. Mastromatteo, A. Conte, M.A Del Nobile, Trends Food Sci. Tech. 21
583 (2010) 591-598.
- 584 [18] M. Vallet-Regí, J.C. Doadrio, A.L. Doadrio, I. Izquierdo-Barba, J. Pérez-Pariente, Solid State
585 Ionics 172 (2004) 435–439
- 586 [19] E. Ghedini, M. Signoretto, F. Pinna, V. Crocellà, L. Bertinetti, G. Cerrato, Micropor. Mesopor.
587 Mat. 132 (2010) 258–267
- 588 [20] M. Al Shamsi, M.T. Al Samri, S. Al-Salam, W. Conca, S. Shaban, S. Benedict, S. Tariq, A.V.
589 Biradar, H.S. Penefsky, T. Asefa, A-K. Souid, Chem. Res. Toxicol. 23 (2010) 1796–1805
- 590 [21] W.H. Suh, K.S. Suslick, G.D. Stucky, Y.H. Suh, Prog. Neurobiol. 87 (2009) 133-170
- 591 [22] C. Coll, L. Mondragón, R. Martínez-Máñez, F. Sancenón, M.D. Marcos, J. Soto, P. Amorós, E.
592 Pérez-Payá, Angew. Chem. Int. Ed. 50 (2011) 2138–2140
- 593 [23] N.K. Mal, M. Fujiwara, Y. Tanaka, Nature 421 (2003) 350-353.
- 594 [24] E. Aznar, L. Mondragón, J.V. Ros-Lis, F. Sancenón, M.D. Marcos, R. Martínez-Máñez, J. Soto, E.
595 Pérez-Payá, P. Amorós, Angew. Chem. Int. Ed. 50 (2012) 11172–11175
596
- 597 [25] R. Guillet-Nicolas, A. Popat, J-L. Bridot, G. Monteith, S.Z. Qiao, F. Kleitz, Angew. Chem. Int. Ed.
598 52 (2013) 2318–2322
- 599 [26] Z. Zhao, H. Meng, N. Wang, M.J. Donovan, T. Fu, M. You, Z. Chen, X. Zhang, W. Tan, Angew.
600 Chem. Int. Ed. 52 (2013) 7487-7491
- 601 [27] C. Park, K. Oh, S.C. Lee, C. Kim, Angew. Chem. Int. Ed. 46 (2007) 1455–1457
- 602 [28] Y. Tian, A. Glogowska, W. Zhong, T. Klonisch, M. Xing, J. Mater. Chem. B. 1, (2013) 5264-5272
- 603 [29] Y. Jiao, Y. Sun, B. Chang, D. Lu, W Yang, Chemistry 19 (2013) 15410-15420.
- 604 [30] K. Patel, S. Angelos, W.R. Dichtel, A. Coskun, Y-W. Yang, J.I. Zink, J. F. Stoddart, J. Am. Chem.
605 Soc. 130 (2008) 2382–2383
- 606 [31] A. Agostini, L. Mondragón, A. Bernardos, R. Martínez-Máñez, M.D. Marcos, F. Sancenón, J.
607 Soto, A. Costero, C. Manguan-García, R. Perona, M. Moreno-Torres, R Aparicio-Sanchis, J.R.
608 Murguía, Angew. Chem. Int. Ed. 51 (2012) 10556-10560

- 609 [32] E. Climent, A. Bernardos, R. Martínez-Mañez, A. Maquieira, M.D. Marcos, N. Pastor-Navarro,
610 R. Puchades, F. Sancenón, J. Soto, P. Amorós, *J. Am. Chem. Soc.* 131(2009) 14075-14080
- 611 [33] L.L. Li, M. Xie, J. Wang, X. Li, C. Wang, Q. Yuan, D.W. Pang, Y. Lu, W. Tan, *Chem. Commun.* 49
612 (2013) 5823-5825
- 613 [34] A. Bernardos, E. Aznar, C. Coll, R. Martínez-Mañez, J.M. Barat, M.D. Marcos, F. Sancenón, A.
614 Benito, J. Soto, *J. Control Release* 131 (2008) 181-189
- 615 [35] A. Bernardos, L. Mondragón, E. Aznar, M.D. Marcos, R. Martínez-Mañez, F. Sancenón, J. Soto,
616 J.M. Barat, E. Pérez-Payá, C. Guillem, P. Amorós, *ACS nano* 4 (2011) 6353-6368.
617
- 618 [36] C.H.M Versantvoort, A.G. Oomen, E. Van de Kamp, C.J.M. Rompelberg, A.J.A.M. Sips, *Food*
619 *Chem. Toxicol.* 43 (2005) 31-40
- 620 [37] R. Póo-Prieto, E. Alonso-Apperte, G. Varela-Moreiras, J. I. Breving 117 (2011) 188–194
- 621 [38] Z Wu, X.X. Li, C.Y. Hou, Y. Qian, *J. Chem. Eng. Data* 55 (2010) 3958– 3961
- 622 [39] A.C. Moffat, Pharm. Press, London, 1986
623
- 624 [40] R. Casasús, E. Climent, M.D. Marcos, R. Martínez-Mañez, F. Sancenón, J. Soto, P. Amorós, J.
625 *Am. Chem. Soc.* 130 (2008) 1903-1917
- 626 [41] N. Kupferschmidt, X. Xia, R.H. Labrador, R. Atluri, L. Ballell, A.E. Garcia-Bennett, *Nanomed.* 8
627 (2013) 57-64